Aggregated power profile of a large network of refrigeration compressors following FFR DSR events

Ibrahim M Saleh
University of Lincoln
United Kingdom
isaleh@lincoln.ac.uk

Andrey Postnikov
University of Lincoln
United Kingdom
apostnikov@lincoln.ac.uk

Chris Bingham
University of Lincoln
United Kingdom
cbingham@lincoln.ac.uk

Ronald Bickerton
University of Lincoln
United Kingdom
rbickerton@lincoln.ac.uk

Argyrios Zolotas
University of Lincoln
United Kingdom
azolotas@lincoln.ac.uk

Simon Pearson
University of Lincoln
United Kingdom
spearson@lincoln.ac.uk

ABSTRACT

Refrigeration systems and HVAC are estimated to consume approximately 14% of the UK's electricity and could make a significant contribution towards the application of DSR. In this paper, active power profiles of single and multi-pack refrigeration systems responding DSR events are experimentally investigated. Further, a large population of 300 packs (approx. 1.5 MW capacity) is simulated to investigate the potential of delivering DSR using a network of refrigeration compressors, in common with commercial retail refrigeration systems. Two scenarios of responding to DSR are adopted for the studies viz. with and without applying a suction pressure offset after an initial 30 second shut-down of the compressors. The experiments are conducted at the Refrigeration Research Centre at University of Lincoln. Simulations of the active power profile for the compressors following triggered DSR events are realized based on a previously reported model of the thermodynamic properties of the refrigeration system. A Simulink model of a three phase power supply system is used to determine the impact of compressor operation on the power system performance, and in particular, on the line voltage of the local power supply system. The authors demonstrate how the active power and the drawn current of the multi-pack refrigeration system are affected following a rapid shut down and subsequent return to operation. Specifically, it is shown that there is a significant increase in power consumption post DSR, approximately two times higher than during normal operation, particularly when many packs of compressors are synchronized post DSR event, which can have a significant effect on the line voltage of the power supply.

KEYWORDS
Demand Side Response, retail refrigeration systems, simulation, power profile, National Grid.

1 INTRODUCTION

Power system infrastructures of many countries are coming under increased pressure as the increase demand of consumers and the penetration of renewable power sources have introduced many technical and operational challenges to the grid, e.g. non-stiff renewable induced system imbalance, and peak capacity issues [1]. DSR has been identified as a powerful tool to help mitigate such challenges by encouraging power consumers to reduce demand consumption during peak times [1, 2].

In Germany, for instance, the largest portion of demand side management is provided by combined heat and power (CHP) and storage heating systems [3]. More widely, demand side management storage strategies for end-consumers is investigated in [4]. The UK National Grid has shown great interest in the development and management of the DSR to better match supply and demand. Refrigeration systems and HVAC are estimated to consume approximately 14% of the UK's electricity and could make a substantial contribution towards a DSR strategy [5] due to the inherent thermal energy storage capacity.

The food industry is the UK's largest manufacturing sector, with food retailing alone accounting for ~12 TWh of energy usage per annum, approximately 3.4% of total electrical consumption [6]. The thermal mass of refrigerated food stores in retail supermarkets provides significant potential for short-term energy buffering, allowing it to be a serious contender to support DSR events [1].

Food refrigeration networks comprise of a large number of compressors and cases. One of the largest retailers in the UK have more than 3500 stores and over 100,000 refrigeration cases. However, the application of DSR in the food refrigeration network is a complicated process and

poses significant technical challenges. Primary of these is necessity to control the refrigerators across the entire estate at high speed whilst ensuring sufficient thermal inertia is available to maintain the food temperature within safety boundaries when the power supply of the refrigeration system has to be shed during a DSR event. Systems where the thermal inertia changes rapidly can be of high risk [7, 8]. Optimised supervisory schemes play a vital role in monitoring the local/distributed controllers [1]. Additionally, delivering DSR across the whole of the UK requires a reliable, rapid IT infrastructure to handle large, high bandwidth data streams [9, 10].

2 Demand Side Response Potential and Challenges

The frequency of a distributed power network provides an indication of the balance between demand and generation. When the level of demand exceeds the available supply, the frequency drops (below the nominal 50 Hz in the UK), while frequency increases above 50 Hz when there is a significant drop in the level of demand with respect to the available power generation. Stabilizing the system frequency within a narrow band around 50 Hz is traditionally accomplished either by regulating the available supply or the load demand through frequency response services. This is important not only for frequency balancing, but to also prevent sudden power plant failures, leading to the prospect of power blackouts [11].

A Firm Frequency Response (FFR) mechanism is triggered when the supply frequency drops to/below 49.7 Hz. The first phase of FFR (primary FFR) must rapidly shed load for 30 seconds, whilst during the second phase (secondary FFR) the load must be held off for up to 30 min—see Figure 1.

The impact of a DSR event and the load shedding/shifting on the voltage stability of power networks, and on overall network stability, is investigated in [2, 12]. In particular, the triggering of a DSR event can impact the voltage of the network (amplitude and/or angular), with the level of change depending on the type and size of the load shed and the characteristics and stiffness of the power network.

Previous investigations have identified issues of power synchronization post-DSR, and the impact of generating high transient demands from refrigeration systems [13, 14]. Although protection and control devices can reduce power fluctuations on the system, the overall stability of the grid and minimising the risk of network failure remains an active topic [15, 16]. Other studies have reported that networks of refrigerators can initiate sequential under-frequency events especially after turning off and then returning to normal operation [17]. Moreover, stability can be further degraded by post recovery inrush currents [5]. However, the use of stochastic decentralized control has previously been reported to be of benefit to ameliorate the impact of such power oscillations for small groups of domestic refrigerators, albeit it is a computationally demanding process [11, 18, 19].

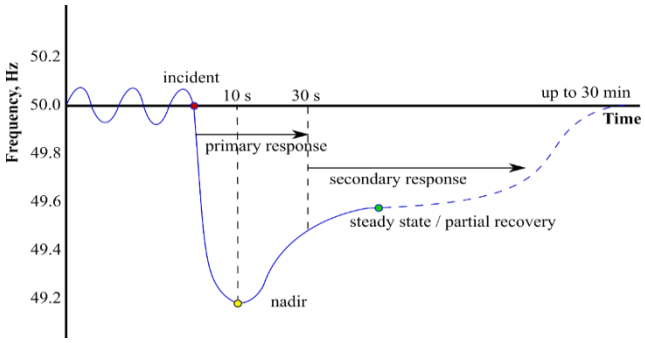

Figure 1: **Overview of Firm Frequency Response National Grid.** (cited form [5]).

Two control approaches in responding to DSR have been previously reported which differ in complexity and implementation costs viz. the load either reacts to changes to the supply in a fully autonomous manner by monitoring the overall system frequency, or, the load responds to an external request initiated, for example, by the grid operator [11]. Most existing business models for DSR focus mainly on improving emergency response or normal operation, with relatively few studies that analyse the impact of DSR during the load recovery interval [12].

Here then, the active power profiles for a single- and multi-pack refrigeration system responding to DSR events are experimentally investigated, and a large population of 300 packs (approx. 1.5 MW capacity) is simulated to investigate the potential of delivering DSR with a network of refrigeration compressors common to the commercial retail sector.

3 Refrigeration System Description

An instrumented refrigeration system representing a small supermarket store is available at the Refrigeration Research Centre at The University of Lincoln. Figure 2 shows the pack of compressors and high temperature cases installed at the test site. The cooling site consists of 13 high temperature HT cases (models Atlas FHGD and Monza FHGD) and 2 low temperature LT cases (model Hockenheim), 2 fan condenser units (model RF-MB102L3H-091-E550) and a pack of Copeland Scroll compressors: 4 identical HT compressors (model

ZB45KCE-TFD) and 2 LT compressors of various sizes (models ZF09K4E-TFD and ZF15K4E-TFD). All compressors operate as fixed volume displacement machines. The compressors receive refrigerant through separate HT and LT suction lines that feed into a common discharge line, thereby providing one-stage compression for refrigerant from both HT and LT cases. Figure 3 shows the schematic diagram of the suction pipeline of the refrigeration system. Case controllers are Danfoss 514B and Danfoss 550. Case control set-points vary from −2 to 1°C for HT cases and −23 °C for LT cases with the nominal acceptable temperature differential set to 2 °C for all cases. Expansion valves are of types AKV10 and TEX for HT and LT cases, respectively. The compressors are controlled by Danfoss 531B to maintain a desired suction pressure in both the HT and LT lines. Suction pressure set-points are 3.4 bar for HT compressors and 0.7 bar for LT compressors.

A multifunction meter (*DIRIS A40/A41*) is installed to measure power consumption every 1s. Power consumption for the 3Φ system is calculated using [20]:

$$P = \sqrt{3} \times (V_{L-L} \times I_L \times Cos\,\emptyset) \quad (1)$$

$$S = \sqrt{3} \times (V_{L-L} \times I_L) \quad (2)$$

$$Q = \sqrt{3} \times (V_{L-L} \times I_L \times sin\,\emptyset) \quad (3)$$

$$Q = \sqrt{(S^2 - P^2)} \quad (4)$$

where, P is active power (Watts), Q is the reactive power (VAR), S is the apparent power (VA), V is the line to line voltage (V), I is the line current (A), φ is the phase shift angle between voltage and current (degree), and $Cos\ \varphi$ is the power factor.

A second testing scenario is also considered to represent a superstore with a large scale refrigeration system (~ 9 times larger than the Refrigeration Centre at the University of Lincoln), comprising of 6 pack of compressors, 4 HT packs operated by 40 compressors, and 2 LT packs operated by 16 compressors, serving 102 HT and LT cases.

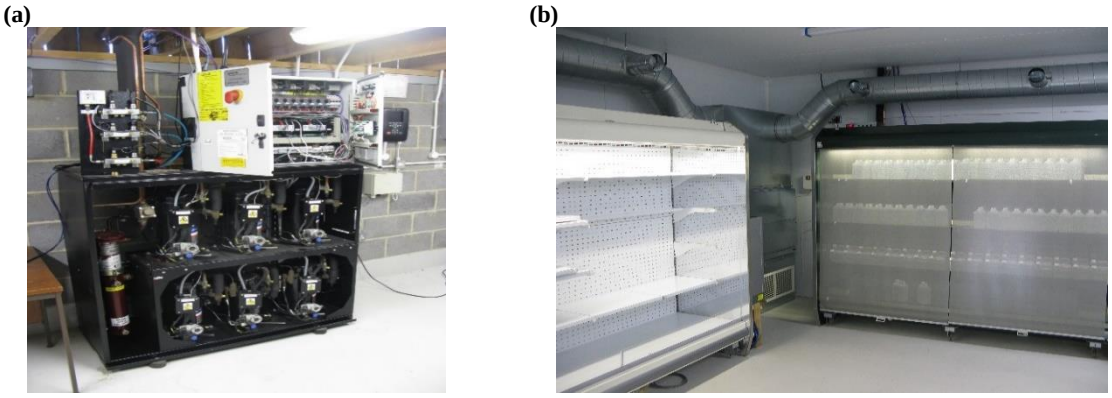

Figure 2: **Refrigeration Research Centre at University of Lincoln; (a) Pack of compressors, (b) Refrigeration cases.**

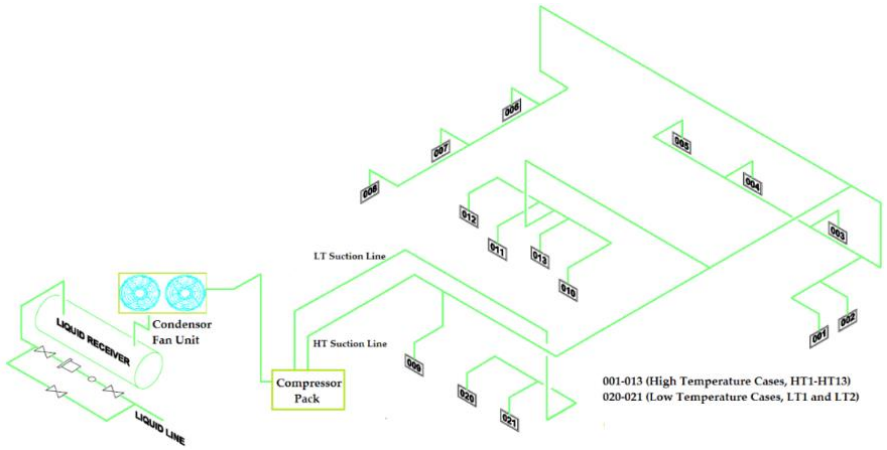

Figure 3: **Schematic diagram of the suction pipeline of the refrigeration system.**

4 Impact of DSR on Power Consumption

The impact of DSR events in the context of the resulting electrical characteristics, is now investigated. The testing procedure is designed to examine different scenarios of system operation in response to FFR DSR. The first scenario considers shutting down the pack of compressors for 30 seconds and then turning them back on, both with and without applying a suction pressure offset for 30 min, and observing system recovery to normal operation. The suction pressure offset is set to 0.6 bar, increasing the reference value of suction pressure from 3.4 to 4.0 bar for the HT system and from 0.7 to 1.3 bar for the LT system. Figure 4 shows the 3Φ active power consumption for a single pack of 4 HT and 2 LT compressors during 24 hours of operation, associated with two DSR events. The first DSR is initiated at 11:19 am, including the application of a pressure offset, as shown in figure 5. The (instantaneous) RMS power consumption can be averaged over the DSR event. This is measured to be ~8 kW. A second DSR event is initiated at 14:18 pm without applying a pressure offset, as shown in figure 6. The average RMS power consumed during this DSR event is 11.54 kW.

Figure 7 shows a 3Φ active power consumption for 6 pack of compressors associated with a further two DSR events. The first is initiated at 13:45 pm, including the application of a pressure offset, as shown in figure 8. The average RMS power consumed during the DSR is 41.5 kW. The second DSR is initiated at 14:45 pm without applying pressure offset, as shown in figure 9. The average RMS power consumed during the DSR is 58.2 kW.

The second and third testing procedures are implemented on a refrigeration system consisting of 6 packs, comprising of 40 HT compressors and 16 LT compressors, plus 102 HT and LT cases. Figure 10 shows the 3Φ active power consumption during 24 hours of operation. The initial DSR event is triggered 09:30 am, by instantaneously (effectively) shutting off the expansion valves off all 102 HT and LT cases. This prevents the flow of refrigerant into the evaporators. Then, after 25 seconds, the compressors are rapidly pulsed OFF and ON (once) to investigate their transient electrical and thermal impact, without applying a suction pressure offset. The recovery to normal operation is then observed. Figure 11 shows the average RMS power consumed during the DSR is 13.6 kW. A second DSR event is initiated at 13:00 pm based on an estimation that there are 75 available candidates of cases that are in a state that can be turned off for 30 minutes without jeopardising food safety. This scenario is depicted in figure 12. The average RMS power consumed during the DSR event is 24.64 kW in this case.

A further DSR is initiated at 11:45 am by instantaneously (effectively) shutting off the expansion valves off all 102 HT and LT cases. Then, after 25 seconds, the compressors are pulsed OFF and ON again, associated with applying suction pressure offset. The recovery to normal operation is then observed. This scenario is presented in figure 13, where the average RMS power consumed during the DSR event is 11.9 kW. When the refrigeration system exits the DSR, the pressure offset is reset to its initial value. This results in more compressors needing to be turned on in order to lower the suction pressure and to supply sufficient refrigerant to the evaporators. Hence, further power is consumed, as shown (in dashed red block) in figure 13.

In summary, the impact of applying a suction pressure offset prior to responding to a DSR event has a significant impact on reducing the power transient (spike) and lowering the average power consumption from 11.54 kW to 8 kW (figures 5 and 6, respectively) for a single pack of compressors, and from 58.2 kW to 41.5 kW (as shown in figures 8 and 9, respectively) for the 6 pack of compressors. This can reduce the frequency of compressor operational duty during the DSR event, thereby lowering the base current requirements of the system during the DSR. Moreover, it will limit the flow of refrigerant in the system and ensure that refrigeration is not disrupted for the cases that cannot be switched off to contribute to the DSR event. This offers the prospect of maintaining the load power shed within specified operational boundaries, and thereby comply with guidelines on Connection Condition, Section 6.3.9 issued by National Grid, which sets out acceptable tolerances on load power transient during a DSR event. Specifically, they should be within a standard deviation of 2.5% of the maximum contracted load-shed value for the aggregated store power profiles [21].

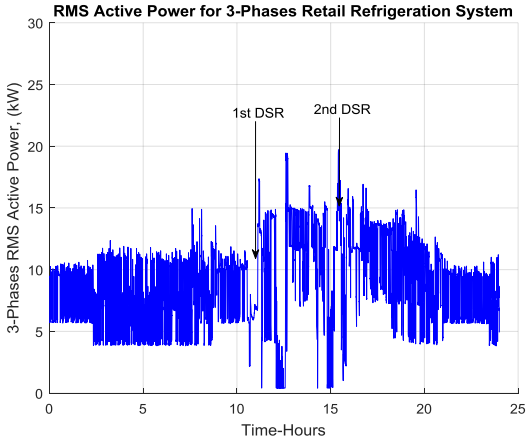

Figure 4: **Power consumption for a single pack of compressors during 24 hours of operation, associated with 2 DSR events.**

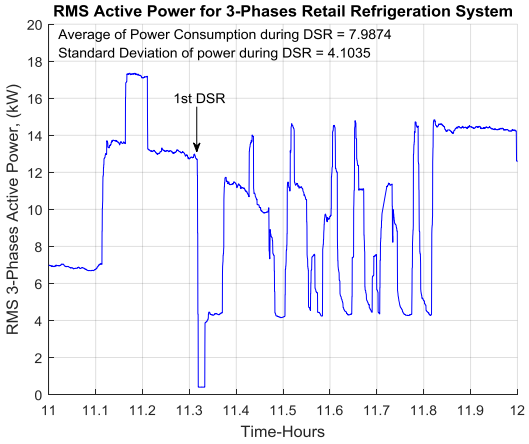

Figure 5: **Power consumption for a single pack of compressors, with a DSR event associated with applying pressure offset.**

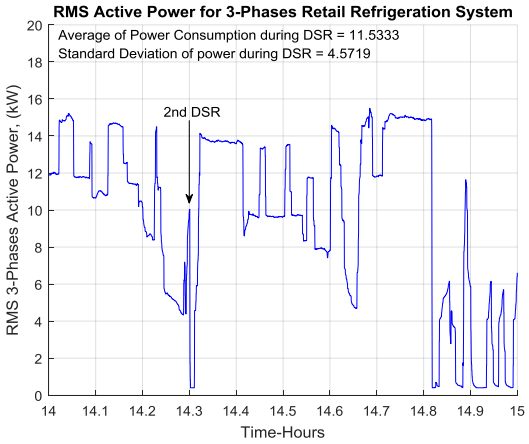

Figure 6: **Power consumption for a single pack of compressors, associated with a DSR event without applying pressure offset.**

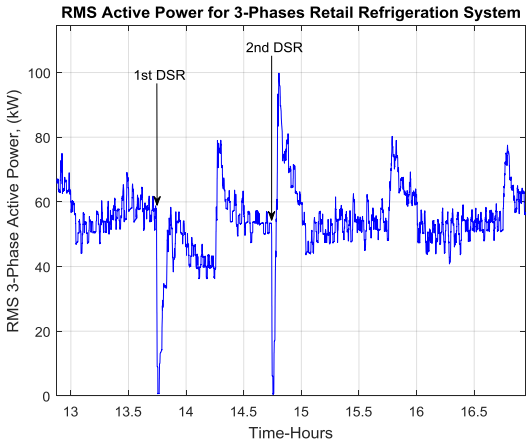

Figure 7: **Power consumption for 6 pack of compressors, associated with 2 DSR events.**

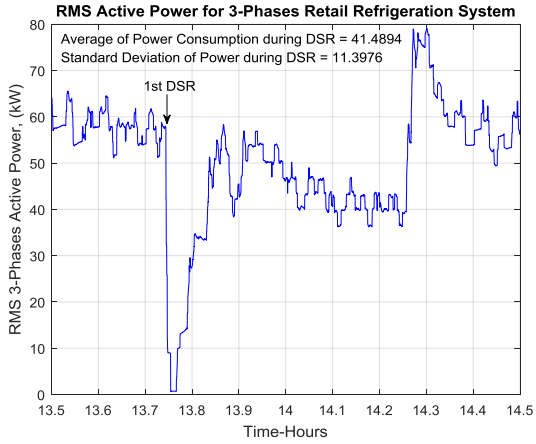

Figure 8: **Power consumption for 6 pack of compressors, associated with applying pressure offset.**

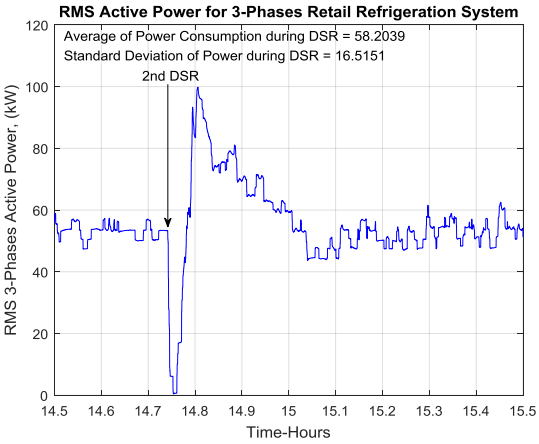

Figure 9: **Power consumption for 6 pack of compressors, without applying pressure offset.**

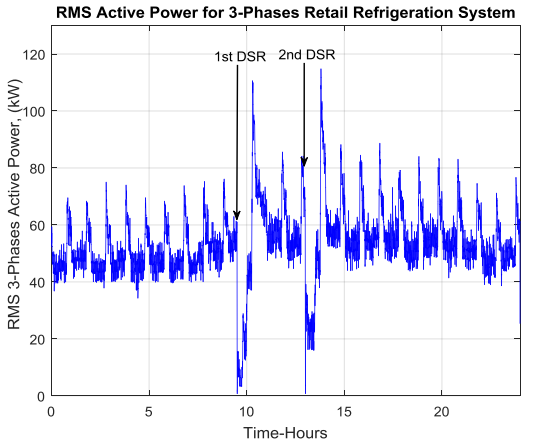

Figure 10: **Power consumption for 6 pack of compressors during 24 hours of operation, with 2 DSR events.**

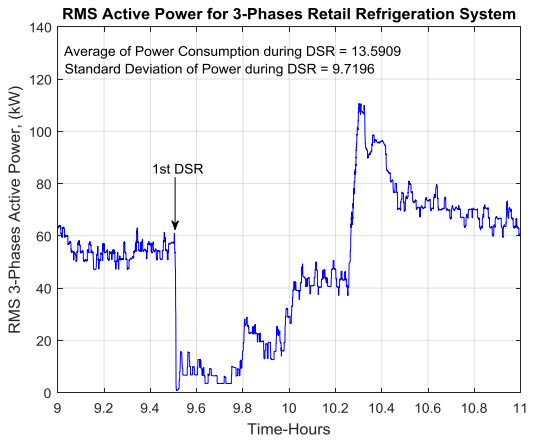

Figure 11: **Power consumption for 6 pack of compressors, based on instantly closing the valve of all cases, then after 25 seconds turning OFF-ON all compressors, without pressure offset.**

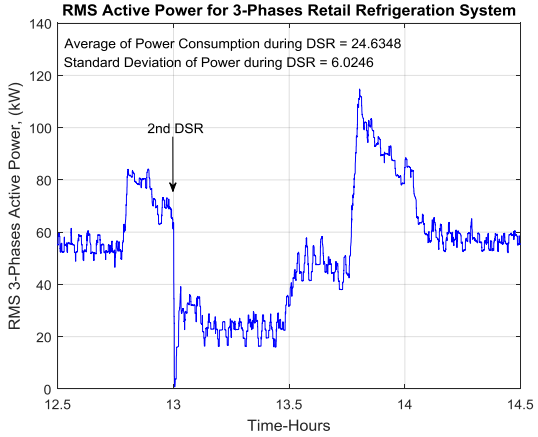

Figure 12: **Power consumption for 6 pack of compressors, with 1 DSR event based on 75 systems available capacity.**

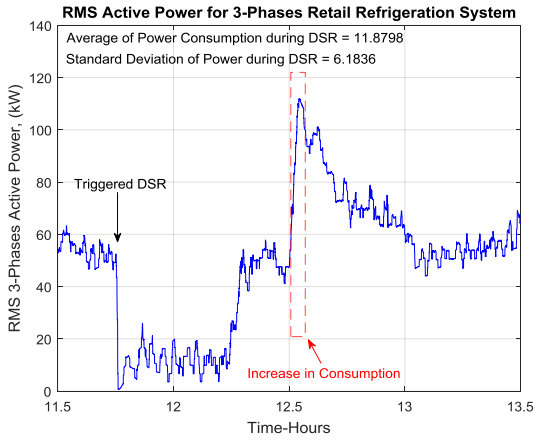

Figure 13: **Power consumption for 6 pack of compressors, based on instantly closing the valve of all cases, then after 25 seconds turning OFF-ON all compressors with applying pressure offset.**

Simulating the operation of 300 packs comprising of 1200 HT compressors and 600 LT compressors, with a load shedding capacity of c.1MW, is now considered. The investigation is based on the thermodynamic-based model of the refrigeration system reported in [22]. A DSR simulation event is based on an estimate of there being ~70% of cases available that can contribute to the DSR for the full 30 min. The DSR is activated by closing only the valves of the cases for 30 min without shutting down the compressors and with no pressure offset applied. The result is shown in figure 14. It can be seen that after 20 min of the DSR, the system cannot maintain power consumption below 500 kW i.e. cannot maintain the original power shed, due to a significant demand for refrigerant due to increasing case temperatures. In contrast, figure 15 shows the power consumption of the simulated 300-pack after a triggered DSR, based on shutting down the compressors for 30s, associated with applying pressure offset and simultaneously closing the valves of the cases for 30 min.

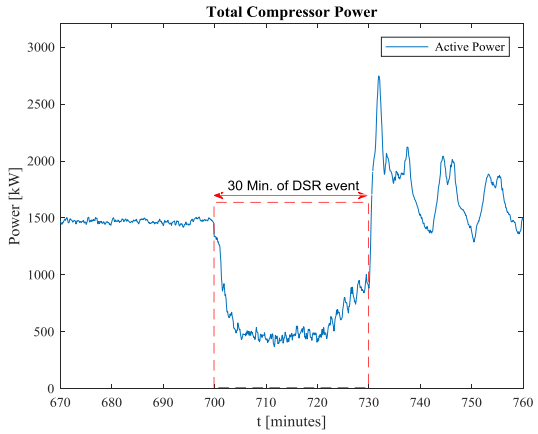

Figure 14: **Power consumption for 300 packs in responding to DSR, based on closing only the valves of the cases for 30 minutes (assumes c.70% available capacity).**

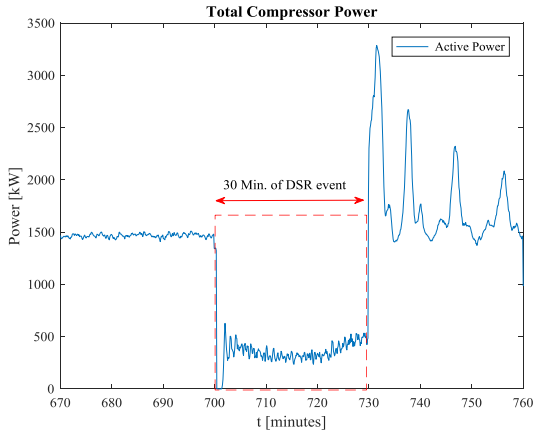

Figure 15: **Power consumption for 300 packs in responding to DSR, based on shutting down the packs for 30 seconds with applying pressure offset, simultaneously closing the valves of the cases for 30 minute (assumes c.70% available capacity).**

Post event (after 30mins); it can be seen that a significant increase in transient power consumption is required amounting to approximately double that of normal operation—see figures (11, 13, 14, and 15), respectively. However, it is greater in situations where a pressure offset is applied, since, post DSR event, the pressure offset is reset to its initial value, as discussed previously.

To examine the impact of the increase in power consumption of the pack of compressors shown in figure 13 (boxed in Red/dash), the 3Φ power supply is modelled in Simulink, figure 16, and for brevity, a single line voltage is considered as being representative of the characteristics. The power system consists of the following primary components:

1. High voltage 11 kV, 50Hz power source with resistive-inductive characteristics. The generator is set to always control the output active- and reactive- power.
2. High voltage 11 kV feeder cable, the distance from the HV distribution substation to the local stepdown transformer is 3 km.
3. Step-down transformer (type Dyn11), where the secondary voltage leads the primary voltage by 30°.
4. Low voltage 433 V feeder cable, the distance from the step down transformer to the site main incomer is 30m.
5. A 3Φ constant resistive-inductive floating Y connection load, with rated active power of 42.5 kW and 26.4 kVAR.
6. A 3Φ dynamic load with the initial rated power of 42.5 kW and 26.4 kVAR.
7. The varying power consumption (P & Q) of the pack of compressors supplied to the dynamic load of the model is imported from the measured power of the experimental refrigeration system consisting of 6 pack of compressors (commensurate with that shown in figure 13).

Parameters, specifications and settings are given in Appendix A, Table A1. Results of the simulations are presented in figure 17 which shows the impact of the increase in power consumption of the compressors on the line voltage of the local power system. Particular note is given to post DSR characteristics, which reduce the line voltage of the local power system. Such characteristics can degrade power system stability especially when many pack of compressors are rapidly synchronised post DSR event. Further investigation is required to examine such an impact from the perspective of the distributed network operator (DNO) of the National Grid.

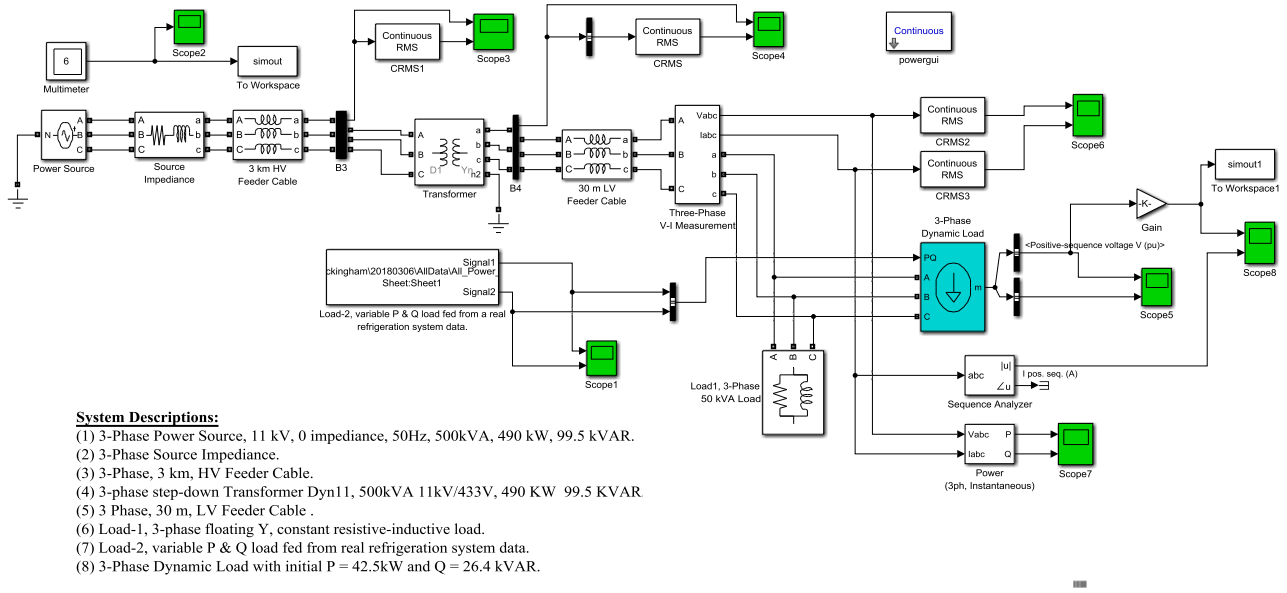

Figure 16: **Simulink block diagram for a three phase power supply system.**

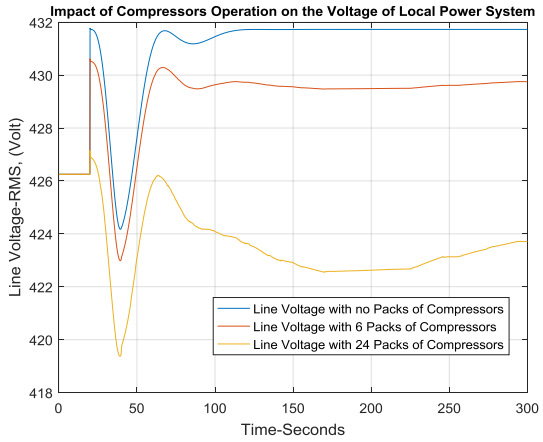

Figure 17: **Impact of the transient power consumption of the compressor pack on the line voltage of the local power system.**

5 CONCLUSIONS

Active power profiles for a single and multi-pack refrigeration system responding to DSRs are investigated experimentally, along with a larger population of 300 packs (approx. 1.5 MW capacity) being simulated to investigate the potential of delivering DSR with a network of refrigeration compressors common to commercial retail refrigeration systems. Various scenarios of responding to DSR are considered in order to examine the power consumption profile of the refrigeration networks.

It is shown that applying a suction pressure offset on the suction line of the refrigeration system prior to responding to a DSR event lowers the transient power requirements, offering the prospect of maintaining power shed levels within minimal operational boundaries. However, it has also been shown that there is a significant increase in power consumption post DSR, approximately two times higher than during normal operation. A trade-off therefore exists between the two operational scenarios in responding to DSR event. Moreover, the increase in the power consumption when many compressor packs are synchronised post DSR event can have a significant effect on supply line voltage. This aspect requires further investigation with a view to realising a scheduled recovery from wide-scale DSR events, and the implications for the DNO of the national Grid.

ACKNOWLEDGMENTS

The authors would like to thank Innovate UK (grant number 54043-400273) for funding this project. Authors also would like to thank Edward Hammond from ECH Engineering and Lee Harpham from IMS Evolve Ltd. for their assistance and guidance during field experiments at the Refrigeration Research Centre.

Appendix A

Table A1. **Values of the parameters, specifications and settings for the components of the Simulink model of power system.**

Rating	Power Source	High Voltage Feeder	Step Down Transformer	Low Voltage Feeder
Voltage	11 kV	-	11 kV/433 V	433 V
Current	39.4 A	-	26.24 A/666.7 A	-
Power Factor	0.98 *	-	0.98 *	-
Apparent Power	750 kVA *	-	500 kVA	-
Active Power	736 kW	-	490 kW	-
Reactive Power	149.3 kVAR	-	99.5 kVAR	-
3-phase Self-Impedance	1 ohm, 1 mH	0.1153 Ohm/km, 1.048 mH/km	-	-
3-phase Mutual-Impedance	-	0.4130 Ohm/km, 3.321 mH/km	-	0.4130 Ohm/km, 3.321 mH/km
3-phase Primary Winding Impedance	-	-	0.024485 Ohm, 1.9244 mH	-
3-phase Secondary Winding Impedance	-	-	6.1714×10^{-5} Ohm, 4.8504×10^{-6} H	-
3-Phase Magnetization Impedance	-	-	4534.3 Ohm, 12.028 H	-

* Assumed values.

REFERENCES

1. Shafiei, S.E., H. Rasmussen, and J. Stoustrup, *Modeling supermarket refrigeration systems for demand-side management.* Energies, 2013. **6**(2): p. 900-920.
2. Kies, A., B.U. Schyska, and L. von Bremen, *The demand side management potential to balance a highly renewable European power system.* Energies, 2016. **9**(11): p. 955.
3. Stadler, I., *Power grid balancing of energy systems with high renewable energy penetration by demand response.* Utilities Policy, 2008. **16**(2): p. 90-98.
4. Atzeni, I., et al., *Demand-side management via distributed energy generation and storage optimization.* IEEE Transactions on Smart Grid, 2013. **4**(2): p. 866-876.
5. Saleh, I.M., et al., *Impact of Demand Side Response on a Commercial Retail Refrigeration System.* Energies, 2018. **11**(2): p. 371.
6. Tassou, S.A., et al., *Energy demand and reduction opportunities in the UK food chain.* Proceedings of the Institution of Civil Engineers-Energy, 2014. **167**(3): p. 162-170.
7. Conte, F., et al., *Stochastic modelling of aggregated thermal loads for impact analysis of demand side frequency regulation in the case of Sardinia in 2020.* International Journal of Electrical Power & Energy Systems, 2017. **93**: p. 291-307.
8. Buzelin, L., et al., *Experimental development of an intelligent refrigeration system.* International Journal of Refrigeration, 2005. **28**(2): p. 165-175.
9. Snijders, C., U. Matzat, and U.-D. Reips, *" Big Data": big gaps of knowledge in the field of internet science.* International Journal of Internet Science, 2012. **7**(1): p. 1-5.
10. Brady, N. and J. Walsh, *Using a Big Data Analytics Approach to Unlock the Value of Refrigeration Case Parametric Data*. ASHRAE Transactions, 2015. **121**: p. 1AAA.
11. Angeli, D. and P.-A. Kountouriotis, *A stochastic approach to "dynamic-demand" refrigerator control.* IEEE Transactions on control systems technology, 2012. **20**(3): p. 581-592.
12. Tang, X. and J.V. Milanović, *Assessment of the impact of demand-side management on distribution network voltage stability.* CIRED-Open Access Proceedings Journal, 2017. **2017**(1): p. 2118-2121.
13. Larsen, L.F., et al. *Synchronization and desynchronizing control schemes for supermarket refrigeration systems*. in *Control Applications, 2007. CCA 2007. IEEE International Conference on*. 2007. IEEE.
14. Kremers, E., et al., *Synchronisation phenomena in electrical systems: emergent oscillation in a refrigerator population*, in *Complex Systems Design & Management*. 2013, Springer. p. 273-284.
15. Short, J.A., D.G. Infield, and L.L. Freris, *Stabilization of grid frequency through dynamic demand control.* IEEE Transactions on power systems, 2007. **22**(3): p. 1284-1293.
16. Stadler, M., et al., *Modelling and evaluation of control schemes for enhancing load shift of electricity demand for cooling devices.* Environmental Modelling & Software, 2009. **24**(2): p. 285-295.
17. Anderson, P.M. and M. Mirheydar, *A low-order system frequency response model.* IEEE Transactions on Power Systems, 1990. **5**(3): p. 720-729.
18. Borsche, T., U. Markovic, and G. Andersson, *A new algorithm for primary frequency control with cooling appliances.* Computer Science-Research and Development, 2016. **31**(1-2): p. 89-95.
19. Kremers, E., J. Marı, and O. Barambones, *Emergent synchronisation properties of a refrigerator demand side management system.* Applied energy, 2013. **101**: p. 709-717.
20. Grigsby, L.L., *The electric power engineering handbook*. 2000: CRC Press.
21. plc, N.G., *CONNECTION CONDITIONS*. 2017, National Grid UK.
22. A. Postnikov, et al., *Modelling of Thermostatically Controlled Loads to Analyse the Potential of Delivering FFR DSR with a Large Network of Compressor Packs*, in *European Modelling Symposium on Mathematical Modelling and Computer Simulation*. 2017: Manchester-UK.